1998

Microminiaturized Immunoassays Using Atomic Force Microscopy and Compositionally Patterned Antigen Arrays

Vivian W. Jones
Iowa State University

Jeremy R. Kenseth
Iowa State University

Marc D. Porter
Iowa State University

Curtis L. Mosher
Iowa State University, cmosher@iastate.edu

Eric Henderson
Iowa State University, telomere@iastate.edu

Anal. Chem. **1998,** *70,* 1233−1241

Accelerated Articles

Microminiaturized Immunoassays Using Atomic Force Microscopy and Compositionally Patterned Antigen Arrays

Vivian W. Jones, Jeremy R. Kenseth, and Marc D. Porter*

Microanalytical Instrumentation Center, Ames Laboratory−USDOE, and Department of Chemistry, Iowa State University, Ames, Iowa 50011

Curtis L. Mosher and Eric Henderson*

Microanalytical Instrumentation Center and Department of Zoology and Genetics, Iowa State University, Ames, Iowa 50011

This paper combines the topographic imaging capability of the atomic force microscope (AFM) with a compositionally patterned array of immobilized antigenic rabbit IgG on gold as an approach to performing immunoassays. The substrates are composed of micrometer-sized domains of IgG that are covalently linked to a photolithographically patterned array of a monolayer-based coupling agent. The immobilized coupling agent, which is prepared by the chemisorption of dithiobis(succinimidyl undecanoate) on gold, is separated by micrometer-sized grids of a monolayer formed from octadecanethiol (ODT). The strong hydrophobicity of the ODT adlayer, combined with the addition of the surfactant Tween 80 to the buffer solution that is used in forming the antibody−antigen pairs, minimizes the nonspecific adsorption of proteinaceous materials to the grid regions. This minimization allows the grids to function as a reference plane for the AFM detection of the height increase when a complementary antibody−antigen pair is formed. The advantageous features of this strategy, which include ease of sample preparation, an internal reference plane for the detection of topographic changes, and the potential for regeneration and reuse, are demonstrated using rabbit IgG as an immobilized antigen and goat anti-rabbit IgG as the complementary antibody. The prospects for further miniaturization are discussed.

Immunoassays play a critical role in clinical, pharmaceutical, and environmental chemistries.[1−3] To such ends, a range of different transduction (e.g., optical,[4−6] amperometric,[7] radiochemical,[8] piezoelectric,[9−13] and capacitive[14,15]) mechanisms have been successfully exploited for the detection of antigen−antibody binding. However, radiochemical, amperometric, and optical

(1) Aga, D. S.; Thurman, E. M. *Immunochemical Technology for Environmental Applications*; ACS Symposium Series 657; American Chemical Society: Washington, DC, 1996.
(2) Diamandis, E. P.; Christopoulos, T. K. *Immunoassay*; Academic Press: San Diego, 1996.
(3) Gosling, J. P. *Clin. Chem.* **1990**, *36*, 1408.
(4) Bright, F. V.; Betts, T. A.; Litwiler, K. S. *Anal. Chem.* **1990**, *62*, 1065.
(5) Tromberg, B. J.; Sepaniak, M. J.; Vo-Dinh, T.; Griffin, G. D. *Anal. Chem.* **1987**, *59*, 1226.
(6) Willumsen, B.; Christian, G. D.; Rozicka, J. *Anal. Chem.* **1997**, *69*, 3482.
(7) Duan, C.; Meyerhoff, M. *Anal. Chem.* **1994**, *66*, 1369.
(8) Chard, T. *An Introduction to Radioimmunoassay and Related Techniques*; Elsevier: Amsterdam, 1987.
(9) Nakanishi, K.; Muguruma, H.; Karube, I. *Anal. Chem.* **1996**, *68*, 1695.
(10) Suleiman, A. A.; Guilbault, G. G. In *Biosensors: Fundamentals, Technologies, and Applications*; Walsdorff, J.-H., Ed.; VCH: New York, 1992; Vol. 17.
(11) Geddes, N. J.; Paschinger, E. M.; Furlong, D. N.; Ebara, Y.; Okahata, Y.; Than, K. A.; Edgar, J. A. *Sens. Actuators B* **1994**, *17*, 125.
(12) Caruso, F.; Rodda, E.; Furlong, D. N. *J. Colloid Interface Sci.* **1996**, *178*, 104.
(13) Ben-Dov, I.; Willner, I.; Zisman, E. *Anal. Chem.* **1997**, *69*, 3506.
(14) Bataillard, P.; Gardies, F.; Jaffrezic-Renault, N.; Martelet, C.; Colin, B.; Mandrand, B. *Anal. Chem.* **1988**, *60*, 2374.
(15) Gebbert, A.; Alvarez-Icaza, M.; Stocklein, W.; Schmid, R. D. *Anal. Chem.* **1992**, *64*, 997.

S0003-2700(97)01125-6 CCC: $15.00
Published on Web 02/26/1998

detection methods generally require the use of labeled receptors, which adds several preparative steps to the overall assay. There are several other issues to consider when these more conventional transduction formats are used. Radiochemical immunoassays, for example, require stringent disposal procedures. In capacitive-based immunoassays, orientation control of an immobilized receptor, and the construction of extremely thin insulating layers for enhancing sensitivity, remain key performance issues. The analytical signal of piezoelectric devices is also affected by the orientation of immobilized receptors, and the response of such devices in liquid environments (e.g., solutions containing bioanalytes) is not fully understood.[12]

Strategies that exploit the microscale characterization capabilities of atomic force microscopy (AFM)[16] have also been investigated for applicability in immunoassays. Recent work has used AFM to detect binding through determinations of the adhesive strengths of antigen−antibody interactions in which the sample is modified with an immobilized antibody and the tip is modified with an immobilized antigen and vice versa.[17,18] Similar studies have been conducted on other ligand−receptor systems,[19,20] with several focusing on the streptavidin−biotin system.[21−24] These determinations are unfortunately affected by nonspecific interactions between a modified probe tip and sample surface, interactions that can have adhesive strengths comparable to those found for the specific interactions between an antigen and its complement antibody.[25] Such determinations require immobilization strategies that result in spatial orientations predisposed to the specific binding interaction between the antigen−antibody pair as a probe tip approaches a sample surface. Indeed, efforts to address this issue are beginning to appear (e.g., the use of a flexible tether on receptors to increase spatial mobility).[26] In all cases, however, a large, statistically valid number of force curves are requisite for gaining an insightful representation of the observed adhesive strengths when using this type of measurement.

In other explorations, the application of AFM as a technique for the detection of antibody−antigen binding has taken a more basic approach by using topographic imaging. This approach relies on the change in the height that results from ligand−receptor binding and, therefore, does not require the use of labeled receptors. In general, height changes of 3−4 nm have been observed as a consequence of adsorption of antigenic IgG to a surface, followed by a similar increase upon antibody−antigen binding.[27−31] Substrates for such studies have been prepared by a lengthy series of surface derivitization steps to fabricate arrays of antibodies on gold or SiO_2,[31] by the use of a maskless photolithographic attachment of photobiotin on glassy carbon,[32] and simply by adsorbing antigens onto mica[30] or a carboxylic acid-terminated self-assembled monolayer.[28] Binding has also been detected through changes in surface roughness,[33] as well as through the topographic observation of antibodies labeled with colloidal gold.[34] In all cases, attempts were undertaken to minimize contributions from nonspecific adsorption.

This paper builds on the above AFM studies by the development of a facile procedure for the creation of square-shaped arrays of immobilized antigens on a gold substrate. Our approach focuses on the construction of micrometer-sized domains of antigens that are covalently linked to a photolithographically patterned array of a monolayer-based coupling agent. As constructed, the immobilized coupling agent, which is prepared by the chemisorption of dithiobis(succinimidyl undecanoate) (DSU) on gold, is separated by micrometer-sized grids of a monolayer formed from octadecanethiol (ODT). Importantly, the strong hydrophobicity of ODT, combined with the addition of the surfactant Tween 80 to the buffer solution that is used in forming the antibody−antigen pairs, minimizes the nonspecific adsorption of proteinaceous materials to the grid regions. This minimization allows the grids to function as a reference plane for the detection of the topographic increase when a complementary antibody−antigen pair is formed. The following sections demonstrate the potential of this approach by using rabbit IgG as an immobilized antigen and goat anti-rabbit IgG as a complementary solution-based antibody. The advantageous features of this strategy, which include ease of preparation, an internal reference plane for the detection of topographic changes, and the potential for regeneration and reuse, are discussed.

EXPERIMENTAL SECTION

Gold Substrate Fabrication. Substrates were prepared using 10 mm × 10 mm silicon wafers ((111) single crystals, Montco Silicon) that were precleaned in an ultrasonic bath for 30 min in water and 30 min in ethanol. Following removal from solution, the substrates were dried using high-purity argon (Air Products) and placed in a vacuum evaporator (Edwards). Next, the substrates were primed with a thin layer (15 nm) of chromium at 0.1 nm/s followed by the deposition of 300 nm of gold (99.99% purity) at 0.3−0.4 nm/s. The gold-coated substrates were either used immediately upon removal from the evaporator or stored under dry nitrogen. We note that attempts to construct patterned arrays using annealed gold films supported on mica were unsuc-

(16) Binning, G.; Quate, C. F.; Gerber, C. *Phys. Rev. Lett.* **1986**, *56*, 930.
(17) Dammer, U.; Hegner, M.; Anselmetti, D.; Wagner, P.; Dreier, M.; Huber, W.; Guntherodt, H.-J. *Biophys. J.* **1996**, *70*, 2437.
(18) Allen, S.; Chen, X.; Davies, J.; Davies, M. C.; Dawkes, A. C.; Edwards, J. C.; Roberts, C. J.; Sefton, J.; Tendler, S. J. B.; Williams, P. M. *Biochemistry* **1997**, *36*, 7457.
(19) Dammer, U.; Popescu, O.; Wagner, P.; Anselmetti, D.; Guntherodt, H.-J.; Misevic, G. N. *Science* **1995**, *267*, 1173.
(20) Chen, X.; Davies, M. C.; Roberts, C. J.; Tendler, S. J. B.; Williams, P. M. *Langmuir* **1997**, *13*, 4106.
(21) Dammer, U.; Anselmetti, D.; Dreier, M.; Hegner, M.; Huber, W.; Hurst, J.; Misevic, G.; Guntherodt, H.-J. In *Forces in Scanning Probe Methods*; Guntherodt, H.-J., Anselmetti, D., Meyer, E., Eds.; Kluwer Academic Publishers: Dordrecht, The Netherlands, 1995; Vol. 286, p 625.
(22) Lee, G. U.; Kidwell, D. A.; Colton, R. J. *Langmuir* **1994**, *10*, 354.
(23) Ludwig, M.; Dettmann, W.; Gaub, H. E. *Biophys. J.* **1997**, *72*, 445.
(24) Moy, V. T.; Florin, E.-L.; Gaub, H. E. *Science* **1994**, *266*, 257.
(25) Stuart, J. K.; Hlady, V. *Langmuir* **1995**, *11*, 1368.
(26) Hinterdorfer, P.; Baumgartner, W.; Gruber, H. J.; Schilcher, K. *Proc. Natl. Acad. Sci. U.S.A.* **1996**, *93*, 3477.
(27) Ill, C. R.; Keivens, V. M.; Hale, J. E.; Nakamura, K. K.; Jue, R. A.; Cheng, S.; Melcher, E. D.; Drake, B.; Smith, M. C. *Biophys. J.* **1993**, *64*, 919.
(28) Browning-Kelley, M. E.; Wadu-Mesthrige, K.; Hari, V.; Liu, G. Y. *Langmuir* **1997**, *13*, 343.
(29) Mulhern, P. J.; Blackford, B. L.; Jericho, M. H.; Southam, G.; Beveridge, T. J. *Ultramicroscopy* **1992**, *42−44*, 1214.
(30) Quist, A. P.; Bergman, A. A.; Reimann, C. T.; Oscarsson, S. O.; Sundqvist, B. U. R. *Scanning Microsc.* **1995**, *9*, 395.
(31) Morgan, H.; Pritchard, D. J.; Cooper, J. M. *Biosens. Bioelectron.* **1995**, *10*, 841.
(32) Dontha, N.; Nowall, W. B.; Kuhr, W. G. *Anal. Chem.* **1997**, *69*, 2619.
(33) Perrin, A.; Lanet, V.; Theretz, A. *Langmuir* **1997**, *13*, 2557.
(34) Feng, C.-D.; Ming, Y.-D.; Hesketh, P. J.; Gendel, S. M.; Stetter, J. R. *Sens. Actuators B* **1996**, *35*, 431.

cessful because of the delamination of gold from the underlying mica during the processing steps described in the next section.

Monolayer Formation and Photopatterning (Steps 1−3). The preparation of the compositionally patterned monolayers at gold followed a multistep procedure. Step 1 involved the formation of an ODT-derived monolayer by immersing the gold-coated substrates into dilute (1−10 mM) ethanolic solutions of recrystallized ODT (Aldrich) for ∼24 h. These samples were then rinsed extensively with ethanol (Quantum, punctilious grade) and dried under a stream of argon.

Step 2 involved the photopatterning process, and followed the general guidelines described in the literature.[35] The patterns were created by carefully sandwiching a copper transmission electron microscopy (TEM) grid (2000 mesh (hole size, 7.5 μm; bar size, 5.0 μm)) (Electron Microscopy Sciences) between an ODT-coated sample and a quartz plate. A 200-W, medium-pressure mercury lamp (Oriel) was used as the light source. The beam was collimated, reflected off an air-cooled, dichroic mirror (220−260 nm), focused by a fused-silica lens, and passed through the TEM grid before impinging onto the sample. The power at the sample was estimated at 550 mW/cm^2. Irradiation times were ∼20 min. Overall, this process converts the irradiated gold-bound thiolates to various forms of oxygenated sulfur (e.g., RSO_3^-), as determined using X-ray photoelectron spectroscopy (XPS) and secondary ion mass spectrometry,[35] Raman spectroscopy,[36] and laser-induced Fourier transform mass spectrometry.[37] Characterizations in our laboratory using XPS and infrared reflection−absorption spectroscopy (IRRAS) confirm the conclusions of the earlier investigations.[38] Importantly, this processing results in oxygenated forms of sulfur that are readily removed from the sample by rinsing with most organic solvents.[36] After such processing, we have detected via AFM the expected height difference (∼2 nm) for patterned surfaces with ODT in the grids and uncoated gold in the squares.

Step 3 entailed the removal of the sulfonated portion of the adlayer structure by rinsing extensively with distilled, deionized water (Millipore) and with ethanol. After drying under a stream of argon, the samples were immediately immersed into a dilute (0.1−1 mM) ethanolic solution of DSU for ∼12 h; the synthesis of DSU followed a combination of published procedures[39,40] and will be discussed elsewhere.[41] Under these conditions, there was no detectable displacement of the ODT adlayer by solution-based DSU, as determined by IRRAS (detection limit, ∼0.05 monolayer) for a ∼12-h immersion. The combination of these three steps results in a compositionally patterned surface, with a DSU adlayer confined in the squares and the ODT adlayer confined in the grids.

Covalent Immobilization of Rabbit IgG (Step 4). The covalent immobilization of polyclonal rabbit IgG (Pierce) was accomplished by the immersion of the compositionally patterned samples into a 50 mM Delbucco's phosphate buffer (PBS) (Life Technologies) at pH 6.0 with the addition of 1% (v/v) Tween 80 (Aldrich) and 1 mg/mL antibody. Tween 80 is incorporated into the PBS solution to minimize any nonspecific binding of IgG onto the surface.[42] Several different methods were explored in an attempt to eliminate any nonspecific binding of antibodies to the sample surface, including varying the buffer composition and immersion times, the use of ultrasonic cleaning, and the addition of Tween 20;[33] we have found, however, that the use of a solution of 1% (v/v) Tween 80 in PBS was the most effective of the approaches. Investigations using AFM in an in situ mode indicated that the immobilization of rabbit IgG at the DSU component of the compositionally patterned surface was effectively complete within ∼90 min, although immersion times were typically much longer (∼12 h) for convenience.

After the immobilization steps were completed, the samples were removed from solution, rinsed with copious amounts of deionized water, and dried under an argon stream. We note that under these conditions there is no detectable hydrolysis of the ester linkage of the DSU monolayer, as determined using IRRAS.

Tests for Viability of Immobilized IgG. Tests for specific and nonspecific binding via AFM were conducted at the patterned array of rabbit IgG-modified samples using 0.1 mg/mL solutions of goat anti-rabbit, goat anti-bovine, and mouse anti-goat IgG in "binding buffer": 100 mM Tris-HCl (pH 7.6), 100 mM NaCl, 15 mM magnesium chloride, and 1% (v/v) Tween 80. Similar tests were conducted using goat anti-rabbit and goat anti-bovine IgG that were both conjugated with fluorescein isothiocyanate (FITC). All of these reagents (Sigma) were used as received.

AFM Imaging. A Multimode NanoScope III AFM (Digital Instruments), equipped with a 150-μm tube scanner, was utilized for the large-scale topography and friction measurements, while a 12-μm tube scanner was used to obtain friction force (f) vs normal load (F_N) plots and friction loops of the DSU and ODT adlayers. All of the images were captured in a contact mode using 200-μm oxide-sharpened Si_3N_4 cantilevers (Nanoprobes) with normal bending and torsional force constants of ∼0.06 and ∼80 N/m, respectively. The conversion of the lateral signal (i.e., the output voltage from the four-quadrant photodiode detector) to f used the sensitivity factor determined for a DSU monolayer at a F_N of 25 nN. Ex situ images were collected under dry nitrogen, whereas a small fluid cell was utilized for in situ experiments. For the in situ experiments, samples containing an immobilized array of antigenic rabbit IgG were directly exposed to the secondary antibody in binding buffer. Fluid was introduced into the AFM cell via pipet injection (Rainin). Images were low-pass and median 5 × 5 filtered for the three-dimensional renditions in Figures 3, 5, and 6. Figure 1 was not filtered.

Fluorescence Imaging. Fluorescence images were acquired using an Odyssey confocal scanning laser microscope (Noran Instruments) in combination with an Axiovert 135 inverted microscope (Zeiss). For fluorescence experiments, the immobilized rabbit IgG arrays were incubated in binding buffer containing

(35) Tarlov, M. J.; Donald R. F. Burgess, J.; Gillen, G. *J. Am. Chem. Soc.* **1993**, *115*, 5305.

(36) Lewis, M.; Tarlov, M.; Carron, K. *J. Am. Chem. Soc.* **1995**, *117*, 9574.

(37) Huang, J.; Hemminger, J. C. *J. Am. Chem. Soc.* **1993**, *115*, 3342.

(38) Upon exposure to UV light under conditions similar to those carried out on the patterned surfaces, samples of ODT examined by XPS showed the appearance of a new peak at a binding energy of 168.2 eV in the S(2p) region. This peak can be assigned to the sulfonate species formed from the UV oxidation of the surface-bound thiolate species. Also, investigations of ODT monolayers using IRRAS revealed the presence of a broad band at ∼1150 cm^{-1} following UV irradiation. This band, in the S−O stretching region, is consistent with the presence of oxygenated forms of sulfur.

(39) Wagner, P.; Hegner, M.; Kernen, P.; Zaugg, F.; Semenza, G. *Biophys. J.* **1996**, *70*, 2052.

(40) Nakano, K.; Taira, H.; Maeda, M.; Takagi, M. *Anal. Sci.* **1993**, *9*, 133.

(41) Jones, V. W.; Kenseth, J. R.; Mosher, C. L.; O'Brien, J. C.; Henderson, E.; Porter, M. D., manuscript in preparation.

(42) Vandenberg, E.; Elwing, H.; Askendal, A.; Lundstrom, I. *J. Colloid Interface Sci.* **1991**, *143*, 327.

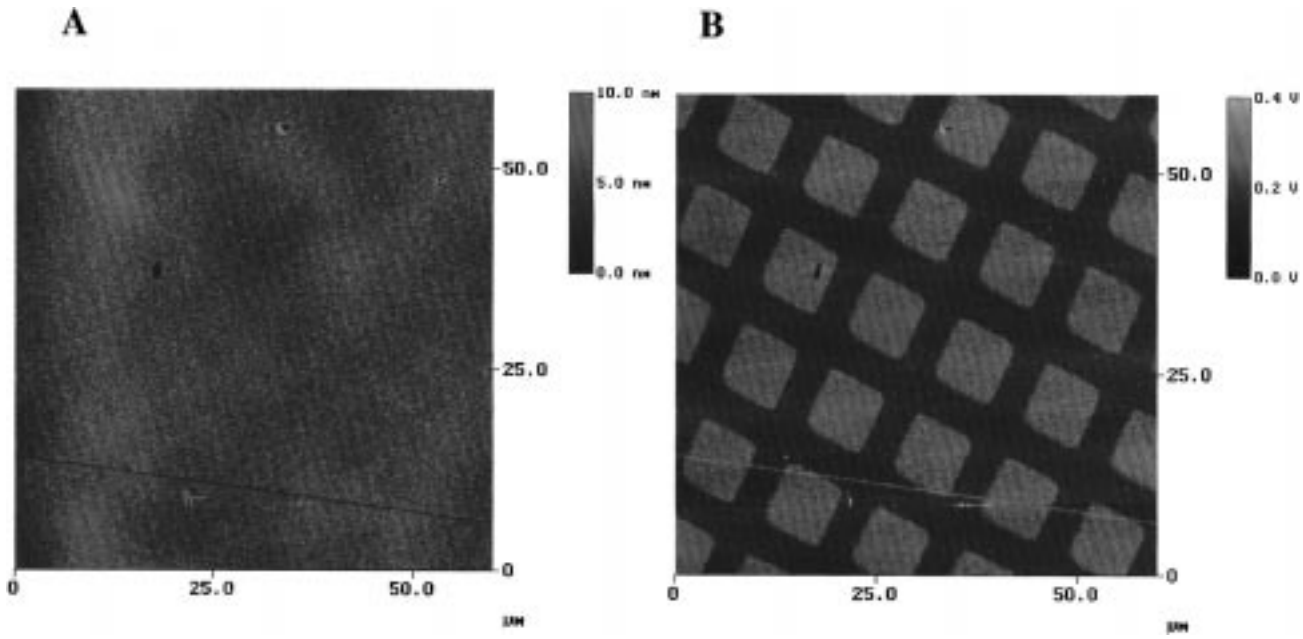

Figure 1. AFM height (A) and friction (B) images (60 μm × 60 μm) of a compositionally patterned surface prepared from steps 1−3 (i.e., a surface modified with an DSU adlayer in the squares and a ODT adlayer in the grids). The images were obtained under a dry nitrogen purge at a F_N of ∼25 nN and a scan rate of 6 Hz.

the FITC-tagged secondary antibody for ∼12 h. After removal from the buffer solution, the samples were rinsed with copious amounts of deionized water and dried under a stream of argon. The samples were protected from light during all preparation steps prior to imaging. The images were acquired using samples immersed in deionized water. Image collection followed a two-step process. First, bright-field images were acquired to establish a focal plane on the sample surface to minimize sample photobleaching. Second, 16 confocal fluorescence images were collected and averaged using 488-nm excitation, a 515-nm low-pass barrier filter (rejection at 488 nm, 4×10^{-4}), and a 25-μm slit width.

RESULTS AND DISCUSSION

Verification of the Construction of Compositionally Patterned Surfaces. This section presents AFM topography (Figure 1A) and friction (Figure 1B) images (60 μm × 60 μm) of the compositionally patterned surface prepared from steps 1−3, i.e., a sample modified with an adlayer of ODT in the grids and an adlayer of DSU in the squares. These images were obtained while the AFM chamber was continuously purged with dry nitrogen. The F_N was ∼25 nN. As is evident, the topography image is devoid of a discernible pattern indicative of the compositional differences expected from step 1. Ellipsometric measurements indicate that the thickness of the DSU component of the patterned adlayer is 1.7−1.9 nm,[39,40] whereas the ODT component of the patterned adlayer (i.e., the grids) is ∼2.2 nm.[43] Thus, the expected difference in height should be 0.3−0.5 nm. We attribute the inability to detect such small differences in height to the simultaneous contact of the tip with both portions of the array in the boundary between the squares and grids.[44] We note that the expected height difference is close to the limit of detection of ∼0.4 nm, as estimated from our recent investigation on the use of friction to map the chemical composition of a partially formed bilayer structure at atomically smooth surfaces.[45] Differences in the compressibility of the two different adlayers may also complicate the imaging process.[46]

In contrast to the topography image in Figure 1A, the concurrent friction image is composed of a periodic array of grids and squares. Both the shape and the dimensions (grids ∼5 μm wide and squares ∼7.5 μm wide) of the pattern are consistent with the expectations of the photopatterns produced using a 2000-mesh TEM grid. In addition, the friction image confirms the compositional difference for the two regions of the patterned surface. There is an easily observable difference in the friction between the squares and the grids, with the squares being higher in friction than the grids. These differences originate, at least in part, from the sensitivity of frictional imaging to the chemical composition of the outermost few angstroms of an interface.[45,47−50]

(43) Bain, C. D.; Troughton, E. B.; Tao, Y.-T.; Evall, J.; Whitesides, G. M.; Nuzzo, R. G. *J. Am. Chem. Soc.* **1989**, *111*, 321−335.

(44) Hayes, W. A.; Kim, H.; Yue, X.; Perry, S. S.; Shannon, C. *Langmuir* **1997**, *13*, 2511.

(45) Green, J.-B. D.; McDermott, M. T.; Porter, M. D.; Siperko, L. M. *J. Phys. Chem.* **1995**, *99*, 10960.

(46) There are three possible and counteracting sources for a difference in compressibility. First, a number of studies have shown that the order of the underlying polymethylene chain in *n*-alkanethiolate monolayers at gold is dependent on chain length,[43,66,67] with the longer chain systems more ordered than the shorter chain systems. The difference in the lengths of the two different adlayers therefore argues that the DSU adlayer may be more compressible that the ODT adlayer. Second, the mismatch in the limited packing density of the succinimidyl end group and polymethylene chain of the DSU adlayer is greater than that for the ODT adlayer.[39,40] Such a situation may compound the difference in the structural ordering of the two different adlayers and further heighten the difference in compressibility. Third, the attractive interactions between neighboring succinimidyl groups in the DSU adlayer are greater than those between the neighboring methyl groups of the ODT adlayer. In this case, the ODT adlayer may be more compressible than the DSU adlayer. The extent of the contributions of each of these interactions is, however, unknown.

(47) Vezenov, D. V.; Noy, A.; Rozsnyai, L. F.; Lieber, C. M. *J. Am. Chem. Soc.* **1997**, *119*, 2006.

As recently demonstrated,[45] the observed friction at the microcontact formed between an AFM probe tip with a high surface free energy (e.g., uncoated Si_3N_4) and a sample with a high surface free energy is greater than that for a sample with a low surface free energy. Wetting characterizations using water as a probe liquid yield an advancing contact angle for an ODT monolayer of 115°[43] and of 50° for a DSU monolayer.[39] It then follows that the friction measured when the tip is in contact with an ODT adlayer (i.e., the grids) should be lower than when the tip is in contact with a DSU adlayer (i.e., the squares).

The observations in Figure 1B are consistent with the general tenets of the above analysis. Determination of friction at the grid and square regions of a patterned surface was conducted by analyzing first the friction loops for samples prepared on an annealed gold substrate, the smoothness of which provides means to assess the AFM-measured friction without contributions from changes in substrate topography.[51] Using the smoother gold samples, the friction found between an uncoated Si_3N_4 probe tip and a DSU adlayer was ~30 nN,[52] whereas that between an uncoated Si_3N_4 tip and an ODT adlayer was less than 2 nN.[53] Together, these data support the creation of the compositionally patterned surface of ODT and DSU at the completion of steps 1−3.

These conclusions are further confirmed by the friction loops shown in Figure 2A and the f vs F_N plots presented in Figure 2B. These data were collected in situ with the same uncoated Si_3N_4 probe tip, with the friction loops obtained at a F_N of ~25 nN. The friction loops for ODT and DSU monolayers show a marked difference in f of ~30 nN, with the ODT adlayer exhibiting a much lower friction than the DSU adlayer. Furthermore, plots of f vs F_N are linear, and the dependence of f at the DSU component is much greater than that at the ODT component. The slope in the case of the former is 1.08 and is 0.12 in the latter. These data demonstrate the sensitivity of f on the chemical identity of the end group of the two different monolayers, supporting the interpretation that the differences in f observed in Figure 1B originate from the spatial difference in the composition of the patterned sample.

Immobilization of Viable Rabbit IgG at the DSU Components of the Spatially Patterned Surface. The last preparation step (i.e., step 4) utilized the samples formed after steps 1−3 to direct the covalent immobilization of rabbit IgG to the DSU portions of the patterned surface. Recent reports have successfully exploited DSU for immobilizing a variety of biomolecules (e.g., antibodies, enzymes, and DNA) for applications as diverse as the construction of impedimetric biosensors,[54] the determination of intermolecular rupture forces,[17,19] and the imaging of

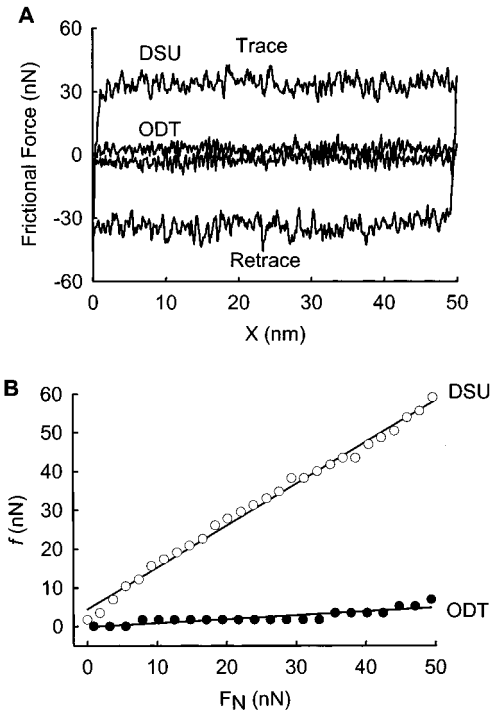

Figure 2. Friction loops (A) and plots of friction force (f) vs normal load (F_N) (B) for DSU and ODT monolayers on Au (111). These images were recorded in deionized water in the center of an atomically flat crystallite. The scan rate was 10 Hz. The friction loops were obtained at a F_N of ~25 nN. The error bars in (B) are approximately three times the size of the symbols.

biomolecules in physiological environments.[55−57] With DSU and structurally related compounds,[39,40,58] the acyl carbon of the succinimidyl ester group is very susceptible to nucleophilic attack by primary amine-containing compounds (i.e., lysine residues of a protein), resulting in the formation of an amide linkage. Because of the large number of lysine residues (60−80) that are distributed throughout the IgG structure,[59] this route to immobilization is likely to yield a wide range of spatially oriented antibodies. It is also possible that an individual IgG molecule may be immobilized by more than one amide linkage. Furthermore, our use of polyclonal IgG ensures some variation among the lysine residues from one antibody to another. The basis of our approach, however, relies on the height change that results from the binding of a large population of immobilized antigens to antibodies where a distribution of orientations is not as critical as in the other noted approaches to immunoassays.

Figures 3 and 4 present evidence for the successful construction of a spatially patterned array of immobilized rabbit IgG. Figure 3A is an AFM topographic image (40 μm × 40 μm) and cross-sectional profile for a patterned surface of ODT and DSU that was subsequently modified with rabbit IgG. The correspond-

(48) Noy, A.; Frisbie, C. D.; Rozsnyai, L. F.; Wrighton, M. S.; Lieber, C. M. *J. Am. Chem. Soc.* **1995**, *117*, 7943.
(49) Frisbie, C. D.; Rozsnyai, L. F.; Noy, A.; Wrighton, M. S.; Lieber, C. M. *Science* **1994**, *265*, 2071.
(50) Wilbur, J. L.; Biebuyck, H. A.; MacDonald, J. C.; Whitesides, G. M. *Langmuir* **1995**, *11*, 825.
(51) McDermott, M. T.; Green, J.-B. D.; Porter, M. D. *Langmuir* **1997**, *13*, 2504.
(52) Wang, J.; Kenseth, J. R.; Jones, V. W.; Green, J.-B. D.; McDermott, M. T.; Porter, M. D. *J. Am. Chem. Soc.* **1997**, *119*, 12796.
(53) The presence of monolayer quantities of adsorbed water on the sample surface can have a significant effect on the adhesion between the tip and sample, which in turn can contribute to the measured friction.[47]
(54) Nakano, K.; Taira, H.; Maeda, M.; Takagi, M. *Trans. Mater. Res. Soc. Jpn.* **1994**, *15A*, 635.
(55) Wagner, P.; Zaugg, F.; Kernen, P.; Hegner, M.; Semenza, G. *J. Vac. Sci. Technol. B* **1996**, *14*, 1466.
(56) Wagner, P.; Kernen, P.; Hegner, M.; Ungewickell, E.; Semenza, G. *FEBS Lett.* **1994**, *356*, 267.
(57) Hegner, M.; Dreier, M.; Wagner, P.; Semenza, G.; Guntherodt, H. J. *J. Vac. Sci. Technol. B* **1996**, *14*, 1418.
(58) Frey, B. L.; Corn, R. M. *Anal. Chem.* **1996**, *68*, 3187.
(59) Wimalasena, R. L.; Wilson, G. S. *J. Chromatogr.* **1991**, *572*, 85.

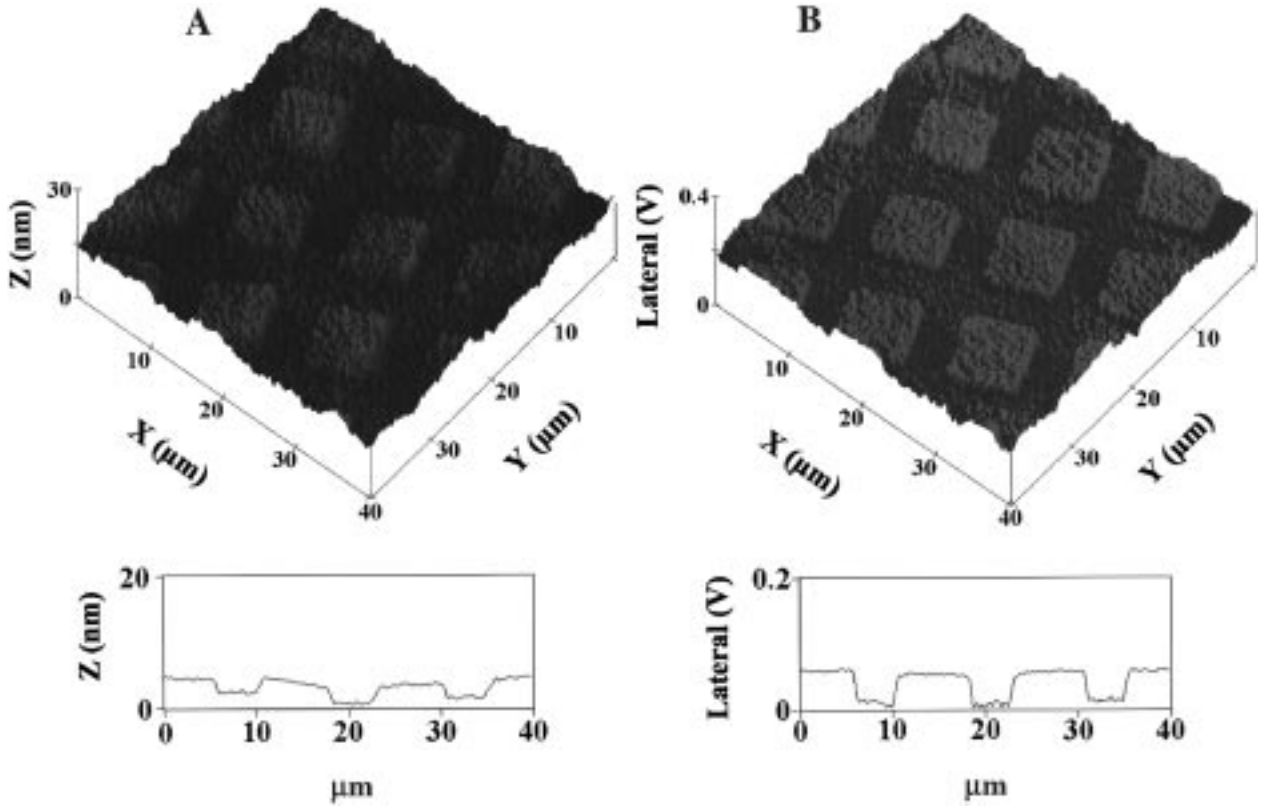

Figure 3. AFM height (A) and friction (B) images (40 μm × 40 μm) obtained under a dry nitrogen purge following the immobilization of rabbit IgG onto the DSU adlayer of the patterned array (i.e., step 4). The cross-sectional analysis was performed by averaging the individual line scans contained in the area of a single row of the array. The images were obtained at a F_N of ~2 nN and a scan rate of 6 Hz.

ing friction image is presented in Figure 3B. Both images, which were acquired under dry nitrogen at a F_N of ~2 nN, exhibit a clearly identifiable pattern of squares and grids. The height for the resulting rabbit IgG adlayer in the squares is 3−4 nm larger than the ODT adlayer in the grids. Importantly, this range of height increase is in reasonable agreement with previously reported findings,[27−31,60] indicating the successful creation of a patterned array of antibodies. The differences in friction are also consistent with the expected differences in the composition of the two components for the patterned surface.[61]

Interestingly, we have found that the detected height differences are dependent on the imaging conditions, as well as on the imaging mode.[41] As expected, the height change when these samples are imaged in liquid (i.e., hydrated) is 30−40% larger than that detected for samples imaged under dry nitrogen (i.e., dehydrated). Thus, in view of the clear increase in the sensitivity to the detection of a height change, the subsequent images were obtained for samples in situ (i.e., in PBS). We have also observed that the detected height changes after immobilization of the antibodies were consistently larger when imaging with the tapping mode than when imaging with the contact mode, although the factors that give rise to this observation, as discussed by others,[62] are not fully understood.

Evidence for the viability of the immobilized array of rabbit IgG is presented in Figure 4 using confocal scanning laser fluorescence microscopy. Figure 4A is an in situ image in deionized water (90 μm × 190 μm) obtained after the exposure of a rabbit IgG array to a specific (i.e., goat anti-rabbit) secondary antibody tagged with FITC. This image exhibits a well-defined fluorescent pattern of 7.5-μm squares that are separated by nonfluorescent grids. This finding indicates (1) that Step 4 results in the immobilization of an array of viable rabbit IgG and (2) that there is no observable nonspecific adsorption of the FITC-tagged antibody on the grids. We attribute the latter observation to the presence of the Tween 80 surfactant (1% v/v) in the buffer solution. As inferred earlier, attempts to immobilize rabbit IgG without the presence of Tween 80 yielded samples where a substantial amount of nonspecific adsorption was detected in the ODT portion of the patterned surface (i.e., the grids) via the fluorescence of FITC-tagged antibodies in the grids.[63] This observation also demonstrated that there was no detectable difference in the possible

(60) Sarma, V. R.; Silverton, E. W.; Davies, D. R.; Terry, W. D. *J. Biol. Chem.* **1971**, *246*, 3753.

(61) We also have evidence from characterizations using IRRAS which, though less defined, supports the covalent immobilization of IgG to DSU. The presence of new amide stretches that would arise from the covalent attachment of IgG to DSU is overwhelmed by the amide bands present in the native antibody. However, we have seen a clear decrease in the carbonyl stretches associated with the succinimidyl moiety, which in turn indicates the cleavage of the succinimidyl ring from the chain. This observation, in turn, suggests that a covalent linkage is formed between the antibody and DSU since we do not detect any hydrolysis of the end group upon exposure to solutions devoid of antibody.

(62) Fritz, M.; Radmacher, M.; Cleveland, J. P.; Allersma, M. W.; Stewart, R. J.; Gieselmann, R.; Janmey, P.; Schmidt, C. F.; Hansma, P. K. *Langmuir* **1995**, *11*, 3529.

(63) It is possible to scrape nonspecific adsorbents off the ODT grid region in these cases with the probe tip by applying a higher normal force while imaging (F_N ~40 nN). Under these scanning forces, the bound protein regions remain viable. This observation further supports the concept that the antibodies are covalently linked to the surface.

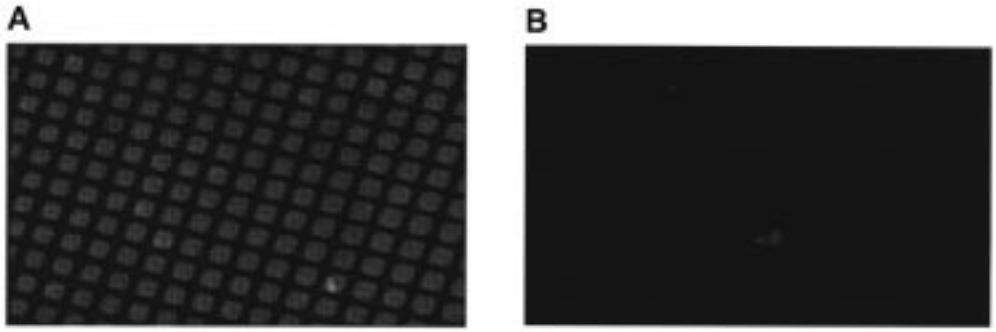

Figure 4. Fluorescence images (90 μm $\times$ 190 μm) of a rabbit IgG array after the addition of goat anti-rabbit (A) or goat anti-bovine FITC-tagged secondary antibodies (B). Images were obtained under deionized water.

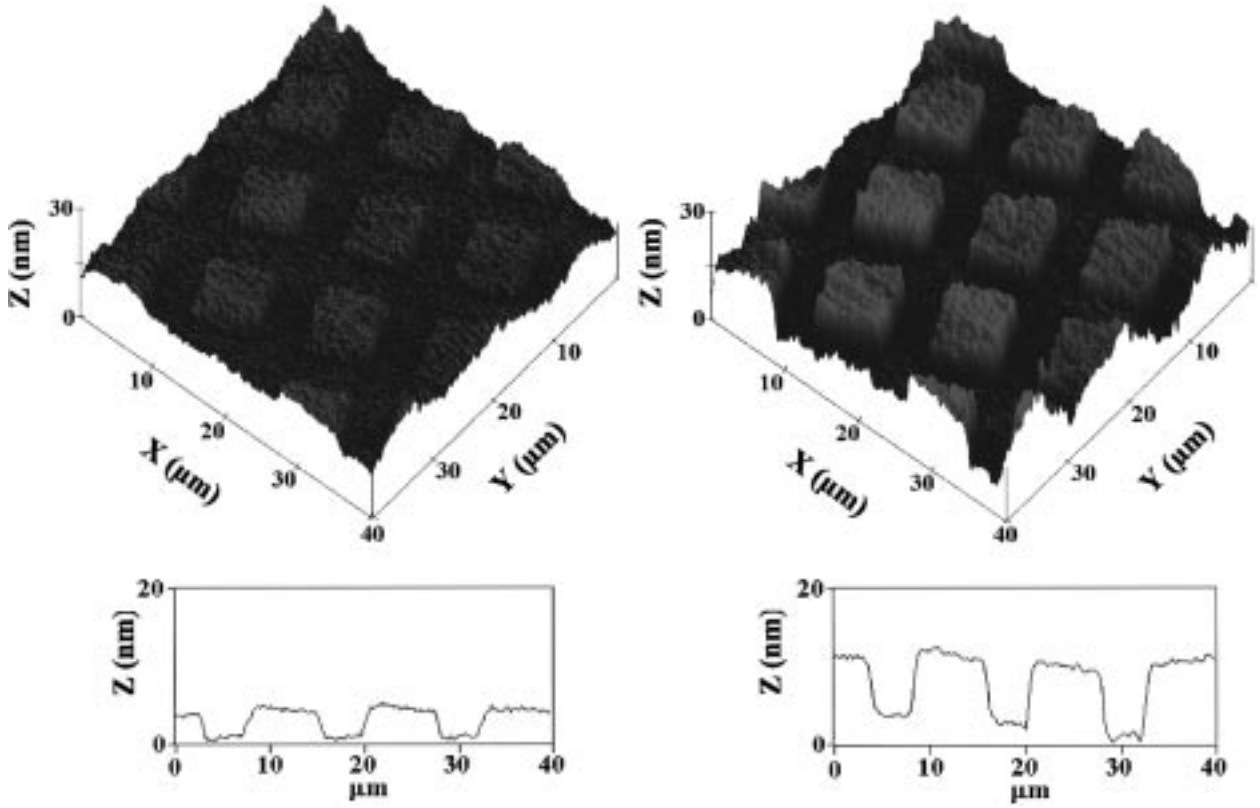

Figure 5. AFM height images (40 μm $\times$ 40 μm) of a rabbit IgG array in (A) 50 mM PBS and 1% (v/v) Tween 80 and in (B) binding buffer with 0.1 mg/mL goat anti-rabbit IgG and 1% (v/v) Tween 80. The cross-sectional analysis was performed by averaging the individual line scans contained in the area of a single row of the array. The images were obtained at a F_N of ~2 nN and a scan rate of ~6 Hz.

quenching of an adsorbed fluorophore on the two portions of the patterned sample.

In contrast to Figure 4A, the in situ image in Figure 4B (90 μm $\times$ 190 μm) was obtained after the exposure of rabbit IgG to a nonspecific (i.e., goat anti-bovine) secondary antibody tagged with FITC. The fluorescence image for this control experiment appears dark under the same illumination conditions used for collecting the image in Figure 4A, indicative of the lack of any detectable nonspecific adsorption of the goat anti-bovine IgG at the patterned array. Taken together, these data in Figures 3 and 4 support the construction of a viable, compositionally patterned array of covalently immobilized rabbit IgG antibodies that can, as shown in the next section, be effectively utilized for a microminiaturized, AFM-based immunoassay.

Height-Based Immunoassays. Finally, we demonstrate the utility of combining the topographic imaging capability of AFM with our compositionally patterned array of rabbit IgG as an approach to performing immunoassays. The in situ images (40 μm $\times$ 40 μm) and accompanying cross-sectional profiles in Figures 5 and 6 present the results of such experiments. The images on the left side of both figures were taken for an array that has rabbit IgG immobilized in the squares and ODT in the grids with the AFM cell filled with PBS solution. The image on the right side of Figure 5 was collected after exposing the sample to a solution of a specific secondary antibody (i.e., 0.1 mg/mL goat anti-rabbit IgG in binding buffer with 1% (v/v) Tween 80) in the sample cell. Conversely, the image on the right of Figure 6 was obtained after exposure to a solution of a nonspecific secondary antibody (i.e., 0.1 mg/mL of goat anti-bovine IgG in binding buffer with 1% (v/v) Tween 80) in the cell. All the images were collected at a F_N of ~2 nN. The images in Figure 5 show that the height of the squares, measured relative to that of the ODT adlayer in the grids,

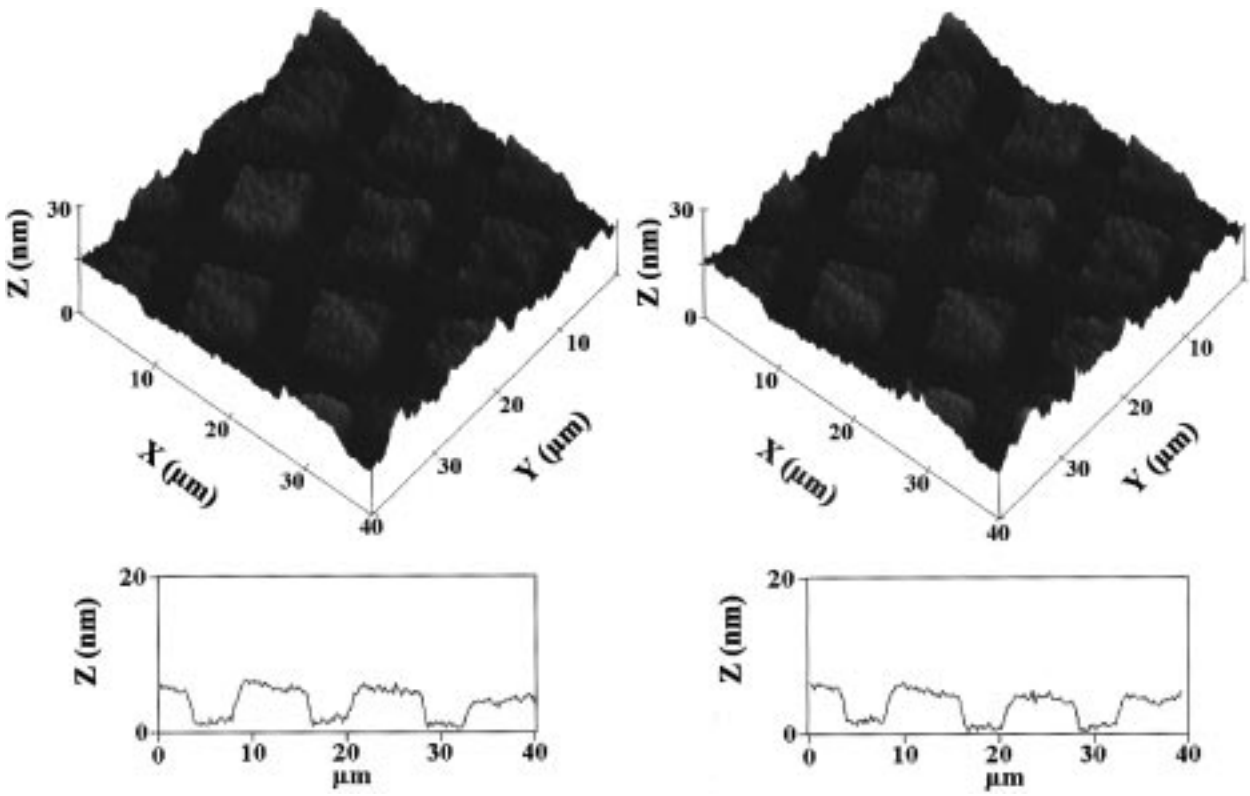

Figure 6. AFM height images (40 μm × 40 μm) of a rabbit IgG array in (A) 50 mM PBS and 1% (v/v) Tween 80 and in (B) binding buffer with 0.1 mg/mL goat anti-bovine IgG and 1% (v/v) Tween 80. The cross-sectional analysis was performed by averaging the individual line scans contained in the area of a single row of the array. The images were obtained at a F_N of ~2 nN and a scan rate of ~6 Hz.

effectively doubles to ~8.5 nm upon the introduction of the solution containing the specific secondary antibody. Furthermore, real-time monitoring reveals that the increase in height appears to be complete within 5 min, which indicates that the binding between the immobilized antigen and solution-based antibody occurs rapidly.[28] Overall, these results are diagnostic of the rapid formation of complementary antigen−antibody pairs within each of the IgG modified elements of the array.

The control experiment represented by the in situ images in Figure 6 confirms that the observed height changes in Figure 5 are the result of specific binding and not nonspecific binding. The height difference between the grids and squares is indistinguishable before (~4.1 nm) and after (~4.2 nm) the exposure of the immobilized array of rabbit IgG to the solution of goat anti-bovine IgG in binding buffer with 1% (v/v) Tween 80. The sample was monitored for several hours with no observable increase in height. Experiments using a solution of mouse anti-goat IgG in binding buffer with 1% (v/v) Tween 80, which is a nonspecific secondary antibody for rabbit IgG, also failed to exhibit a detectable increase in height after several hours. The combined weight of the findings in Figures 5 and 6 therefore demonstrate the potential of this strategy for microminiaturized immunoassays using AFM.

In addition to the above results, a preliminary study supports the possible regeneration and reuse of our patterned arrays. This experiment was conducted by rinsing a rabbit IgG array that was coupled to goat anti-rabbit IgG with a solution of 100 mM glycine-HCl (pH 2.4). As described previously,[9] this processing effectively breaks the antigen−antibody pair and leaves the rabbit IgG array intact for potential reuse. Topographic imaging after exposure to the glycine-HCl solution showed the original rabbit IgG array was still present. Further experiments are now being conducted to examine more extensively the repeatability of this process.

CONCLUSIONS

This paper has demonstrated the potential of combining the topographic imaging capabilities of AFM with a compositionally patterned micrometer-sized array of immobilized antigens as a rapid methodology for immunoassays. Central to our approach is the use of a hydrophobic component in the patterned array that, when combined with the addition of Tween 80 to the incubation solution, minimizes the nonspecific adsorption of proteinaceous materials. This minimization provides a topographic reference plane in the patterned array for the detection of the height increase that results when an antibody binds specifically to its immobilized antigen. Though more extensive testing is needed, preliminary results also show that these arrays can be regenerated and reused. Indeed, we attribute the ability to regenerate readily our array to the stability that results from the covalent tethering of the immobilized antigen through the gold-bound DSU coupling agent.

On the basis of these results, it is worthwhile to examine some of the issues requisite to realize the potential of our approach to immunoassays and other types of clinical diagnostics. Our findings, as well as those of others,[27,28,30,64,65] clearly show that AFM

(64) Fritz, J.; Anselmetti, D.; Jarchow, J.; Fernandez-Busquets, X. *J. Struct. Biol.* **1997**, *119*, 165.
(65) Droz, E.; Taborelli, M.; Descouts, P.; Wells, T. N. C.; Werlen, R. C. *J. Vac. Sci. Technol. B* **1996**, *14*, 1422.
(66) Camillone, N., III; Leung, T. Y. B.; Schwartz, P.; Eisenberger, P.; Scoles, G. *Langmuir* **1996**, *12*, 2737.
(67) Porter, M. D.; Bright, T. B.; Allara, D. L.; Chidsey, C. E. D. *J. Am. Chem. Soc.* **1987**, *109*, 3559.

has more than sufficient sensitivity to detect the height increase that occurs from the formation of a single antibody−antigen pair. Thus, the issue of adequate sensitivity has been addressed. A more critical issue, then, is sample density. A typical AFM can scan an area of more than 100 μm^2 in 1−5 min. Thus, for an array such as those described here, with 5-μm squares and 2-μm-wide grid bars, the AFM could interrogate ∼200 individual addresses in a few minutes. Conventional photolithography (∼0.3-μm resolution) for pattern fabrication could generate an array containing over 100 000 molecular addresses. Thus, it appears that the limiting factor is the development of sophisticated preparative approaches to the construction of an array where each element is compositionally unique. We are presently considering strategies to this end that are based on pattern development using both photolithography and AFM-based patterning concepts, the latter having the potential to create arrays with densities even greater than those using conventional photolithography.

There is also a need to develop data analysis methods that are designed specifically for processing the topographic differences of an array before and after exposure to a serum sample and to delineate correlations between height changes and sample concentration. This issue should be readily addressed by the modification of the software presently used in such instruments by adding capabilities for address indexing and height threshold discrimination. The latter is, in fact, already partially developed in the software packages for most AFM instruments which include techniques such as Bearing Analysis. The success of these early efforts to integrate AFM technology with chemical and molecular analyses strongly suggests that continued work in this area is likely to culminate in the creation of a rapid, high-throughput technology with wide application in areas such as immunodiagnostics and drug discovery.

ACKNOWLEDGMENT

We express our appreciation for the helpful discussions with J. C. O'Brien during the preparation of the manuscript. This work was supported in part by the National Science Foundation (Grant BIR-9601789), the Microanalytical Instrumentation Center and the Laboratory for Cellular Signaling of Iowa State University, and the Office of Basic Energy Science, Chemical Sciences Division of the U.S. Department of Energy. V.W.J. acknowledges the support of a Postdoctoral Fellowship through the Institute of Physical Research and Technology of Iowa State University. The Ames Laboratory is operated for the U.S. Department of Energy by Iowa State University under Contract W-7405-eng-82.

Received for review October 10, 1997. Accepted December 29, 1997.

AC971125Y